A Short Hairpin DNA Analogous to miR-125b Inhibits C-Raf Expression, Proliferation, and Survival of Breast Cancer Cells

Marco H. Hofmann,[1] Jochen Heinrich,[1] Gerald Radziwil,[1] and Karin Moelling[1,2]

[1]University of Zurich, Zurich, Switzerland and [2]Institute of Advanced Study, Berlin, Germany

Abstract

The noncoding RNA miR-125b has been described to reduce ErbB2 protein expression as well as proliferation and migration of cancer cell lines. As additional target of miR-125b, we identified the c-raf-1 mRNA by sequence analysis. We designed a short hairpin-looped oligodeoxynucleotide (ODN) targeted to the same 3′ untranslated region of c-raf-1 mRNA as miR-125b. The fully complementary ODN antisense strand is linked to a second strand constituting a partially double-stranded structure of the ODN. Transfection of the c-raf-1–specific ODN (ODN-Raf) in a breast cancer cell line reduced the protein levels of C-Raf, ErbB2, and their downstream effector cyclin D1 similar to miR-125b. MiR-125b as well as ODN-Raf showed no effect on the c-raf-1 mRNA level in contrast to small interfering RNA. Unlike miR-125b, ODN-Raf induced a cytopathic effect. This may be explained by the structural properties of ODN-Raf, which can form G-tetrads. Thus, the short hairpin-looped ODN-Raf, targeting the same region of c-raf-1 as miR-125b, is a multifunctional molecule reducing the expression of oncoproteins and stimulating cell death. Both features may be useful to interfere with tumor growth. (Mol Cancer Res 2009;7(10):1635–44)

Introduction

MicroRNAs (miR) are a class of endogenous noncoding single-stranded RNAs ~22 nucleotides (nt) in length, which are incorporated in the RNA-inducing silencing complex (1). RNA-inducing silencing complex and miRs regulate the amount of protein expressed from coding RNAs by translational repression or by cleavage of the target mRNA due to base pairing with the 3′ untranslated region (UTR). MiRs have been linked to essential physiologic processes such as regulation of proliferation, differentiation, and apoptosis (1-4) and to several diseases including cancer (5, 6).

Received 2/2/09; revised 8/7/09; accepted 8/14/09; published OnlineFirst 10/13/09. The costs of publication of this article were defrayed in part by the payment of page charges. This article must therefore be hereby marked *advertisement* in accordance with 18 U.S.C. Section 1734 solely to indicate this fact.

Note: M.H. Hofmann and J. Heinrich contributed equally to this work. Current address for M.H. Hofmann: Roche Diagnostics GmbH, Nonnenwald 2, 82377 Penzberg, Germany. Current address for G. Radziwill: Faculty of Biology, University of Freiburg, Faculty of Biology, 79104 Freiburg, Germany.

Requests for reprints: Karin Moelling, University of Zurich, Gloriastr. 32, 8006 Zurich, Switzerland. Phone: 41-49-172-3274306; Fax: 41-44-7303682. E-mail: moelling@imm.uzh.ch

doi:10.1158/1541-7786.MCR-09-0043

Silencing of gene expression can be mediated by miRs, single-stranded antisense DNA (asDNA), short hairpin-looped oligodeoxynucleotides (ODN), or small interfering RNAs (siRNA; refs. 7-10). These molecules exert different functions. SiRNA and asDNA primarily lead to reduction of mRNA by cleavage, whereas miRs primarily block translation (11-13). Inhibition of translation has also been described for asDNA as secondary effect (14, 15). ODNs are a special class of short hairpin-looped DNAs that can induce cleavage of viral RNAs via a retroviral or cellular RNase H and therefore are active as antiviral agents (16-20).

Only miRs are endogenously expressed and can be deregulated in cancer tissue. Thus, miRs targeted to mRNAs are possible targets for cancer therapy (4, 21, 22). The mitogen-activated protein kinase pathway, composed of the kinases Raf, mitogen-activated protein kinase/extracellular signal–regulated kinase (ERK) kinase, and ERK, controls the proliferation and survival of cells (23). Deregulation of this pathway is characteristic for many human tumors. Accordingly, activating mutants of Raf proteins and upstream elements such as receptor tyrosine kinases and Ras proteins were identified in these tumors (24-28).

Small inhibitory molecules such as asDNA, siRNA, and antibodies have been developed to target the mitogen-activated protein kinase pathway (29). Recently, it has been described that miR-125b, which is downregulated in breast cancer cells, targets the mRNA of erbB2 (3). Overexpression of miR-125b inhibited the proliferation and migration of breast cancer cells (30).

We asked whether Raf proteins might be targets of miRs. We identified by database analysis the 3′UTR of c-raf-1 as a putative target of miR-125b and show here miR-125b–dependent inhibition of C-Raf protein expression. Based on this information, we designed a Raf-specific hairpin-loop-structured ODN (ODN-Raf), one arm of which was fully complementary to c-raf mRNA. Here we show that ODN-Raf can reduce the expression of C-Raf and ErbB2. In addition, ODN-Raf was able to induce cell death, which we did not observe with miR-125b or siRNA-Raf. We speculate that structural properties of the ODN-Raf contribute to this effect, for example, the ability to form G-tetrads. Thus, ODN-Raf is a multifunctional molecule that reduces proliferation by inhibition of oncogene expression and induces cell death.

Results

Design of a Short Hairpin-Looped ODN Based on miR-125b

Previously, asDNA, siRNA, miR, as well as short hairpin-looped ODNs have been described to silence gene expression

(1, 8, 17, 19, 20, 31, 32). The 3′UTRs of mRNAs are preferred target sites for miRs and play an essential role in translational control and in the stability of transcripts (13, 33). MiR-125b has been recently described to target erbB2 mRNA (30). Using the miRBase sequence database from Sanger (version 4), we identified an additional putative cancer relevant target site for miR-125b in the 3′UTR of c-raf-1 with a score of 15.65 and energy of −21.45 (Fig. 1A).

We asked whether an ODN targeting c-raf-1 mRNA at the same site as miR-125b could mimic such effects. We designed a hairpin-looped ODN of 54 nt containing a fully complementary antisense strand of 25 nt targeting the same site on the 3′ UTR of c-raf-1 as miR-125b (Fig. 1A and B). The antisense strand is linked by four thymidines to a second strand of 25 nt, which itself is partially complementary to the antisense strand. The ODN-Raf antisense strand is also partially complementary to the target site of miR-125b in the 3′UTR of erbB2 mRNA (11 of 26 nt are complementary; Fig. 1A). Both the antisense and the second strand are G-rich. Three nucleotides at both ends and the linker contain phosphorothioate-modified nucleotides to protect against nucleases. Control ODNs used in this study carry an antisense and a second strand noncomplementary to c-raf-1 or erbB2 mRNA. The ODN designated as ODN-G-rich is not complementary to c-raf-1 or erbB2 mRNA but carries five G-tracts and was designed to investigate the potential influence of G-tracts. Various controls were used to show specificity (Fig. 1B).

Effect of miR-125b on C-Raf Protein Expression

We used two human breast cancer cell lines, a noninvasive cell line, MDA-MB-453, and a highly invasive cell line, MDA-MB-231, which have been analyzed in previous studies with miRs (3, 34). MiR-125b expression level in MDA-MB-453 cells is reduced compared with MDA-MB-231 cells (Fig. 2A). C-Raf and ErbB2 are differentially expressed in both cell lines, whereby their higher expression in MDA-MB-453 cells correlated with the reduced miR-125b level (Fig. 2B and C). Transfection of MDA-MB-453 cells with miR-125b led to a 400-fold increase of miR-125b compared with mock-transfected cells (Fig. 2D). As expected, the increase of miR-125b reduced ErbB2 protein levels by 70% compared with mock-transfected cells (Fig. 2B and C). In addition, transfection of miR-125b reduced the levels of C-Raf protein by 50% (Fig. 2E and F). This indicates that miR-125b can target the 3′UTR region of c-raf-1 mRNA as predicted from our *in silico* analysis.

Effect of ODN-Raf and miR-125b on the Expression of C-Raf and Cyclin D1 Proteins

MiRs, asDNA, as well as siRNA can reduce the protein levels expressed from a target gene. The cellular effects of short hairpin-looped ODNs are less well characterized but can affect viral mRNA levels, especially in the presence of a viral RNase H (18-20). We asked what effect on protein expression could be observed after transfection of ODN-Raf. A single transfection of 25 or 50 nmol/L ODN-Raf in MDA-MB-453 cells reduced the levels of C-Raf after 24 hours by 35% and 65%, respectively, compared with mock transfection (Fig. 3A). A similar reduction was also observed for asDNA-Raf and siRNA-Raf (Fig. 3B). The siRNA-Raf was a commercially available validated siRNA (35) against a different target site on c-raf-1 mRNA (Fig. 1A). The quantification of five independent experiments revealed that these reductions were statistically significant (Fig. 3C). Higher concentrations of oligonucleotides up to 500 nmol/L or longer incubation up to 72 hours did not improve the effect further (data not shown). Also, ErbB2 levels were reduced by ODN-Raf (Fig. 3A and B) similarly as by miR-125b (Fig. 2F). AsDNA-Raf decreased ErbB2 but to a lower extent. The reduction of ErbB2 can be explained by the fact that both ODNs are complementary to a stretch of 11 nt in the erbB2 mRNA (Fig. 1A). SiRNA-Raf did not significantly alter ErbB2 expression but was specific for c-raf-1 (Fig. 3B).

The cell cycle regulator cyclin D1 is regulated by both Raf and ErbB2 via the ERK pathway (36, 37). Consistently, ODN-Raf strongly decreased cyclin D1 levels in MDA-MB-453 cells (Fig. 3A and B). Thus, ODN-Raf resulted in a transient reduction of C-Raf, ErbB2, and their downstream effector cyclin D1. Also, in the highly invasive breast cancer cell line MDA-MB-231, transfection of ODN-Raf reduced C-Raf protein expression up to 80% compared with untreated cells, 24 hours after transfection (Fig. 3D). Thus, in two breast cancer cell lines, ODN-Raf inhibited C-Raf expression.

Cholesterol Conjugation of ODNs Can Replace Transfection Reagents

3′-Cholesterol modifications of miRs can lead to enhanced transfection efficiencies and even allow *in vivo* transfections (38, 39). Therefore, we analyzed cholesterol-modified ODN-Raf for an effect on C-Raf levels. Transfection of MDA-MB-453 cells with 50 nmol/L 5′-cholesterol–modified ODN-Raf without transfection reagent did not affect C-Raf level, whereas 500 nmol/L decreased C-Raf level by 65%, similar to 50 nmol/L nonmodified ODN-Raf transfected with Lipofectamine 2000 (Fig. 4). Accordingly, cyclin D1 was similarly reduced under these conditions. This result indicates that 5′-cholesterol–modified ODNs require a 10 times higher concentration of ODN in the absence of a transfection reagent.

Influence of ODN-Raf and miR-125b on C-Raf-1 mRNA Levels

Initially, miRs were thought to negatively regulate protein expression solely by inhibiting mRNA translation (13, 40, 41). However, in recent studies, it has been shown that some miRs could also induce rapid decay of mRNA transcripts (13). Thus far, we have shown that miR-125b and ODN-Raf reduced the level of C-Raf. To test whether transfection of ODN-Raf and miR-125b also affected the mRNA level, we used a commercially available highly sensitive quantitative real-time reverse transcription-PCR (RT-PCR) TaqMan assay for c-raf-1 mRNA. We transfected MDA-MB-453 cells with 50 nmol/L ODN-Raf or miR-125b. Twenty-four hours after transfection, cells were lysed and c-raf-1 mRNA was isolated and analyzed by quantitative real-time RT-PCR and standardized by β-actin mRNA. No significant reduction of c-raf-1 mRNA was observed after transfection of ODN-Raf or miR-125b compared with nontransfected cells (Fig. 5A). As a positive control, we tested siRNA, which is known to act on the

transcriptional level. As expected, siRNA-Raf reduced the level of c-raf-1 mRNA transcripts by 66% compared with the untreated cells. AsDNA-Raf reduced the mRNA level of c-raf-1 by 25% compared with untransfected cells. Moreover, ODN-Raf did not lead to a significantly increased reduction of c-raf-1 mRNA at different time points between 3 and 48 hours when compared with control 186 or untreated cells (Fig. 5B). In conclusion, ODN-Raf and miR-125b do not act by degradation of the c-raf-1 mRNA.

ODN-Raf Can Adopt Higher-Ordered Structures

On transfection with ODN-Raf, MDA-MB-453 cells exhibited a strong cytopathic effect, which was not observed for miR-125b, miR-125b-DNA, siRNA-Raf, and various control ODNs and only weakly for asDNA-Raf (see below). Because ODN-Raf contains four G-tracts (Fig. 1), we tested whether it can form higher-ordered structures. ODN-Raf as well as a control ODN-G-rich, which contains five G-tracts, showed in addition to their major bands (~50 bp), representing the monomer, a second slower-migrating band (Fig. 6A), which was not detectable with the controls 186 and 187. To determine whether these minor bands correspond to G-tetrads, we analyzed their stability in the presence of monovalent cations because G-tetrads are stabilized by Na^+ or K^+, but not by Li^+ (42). Heat denaturation in the presence of Na^+- and K^+-containing buffer maintained the slower-migrating band, which diminished in the presence of Li^+, suggesting a contribution of G-tetrads (Fig. 6B). Even though they are not abundant, they may play a role.

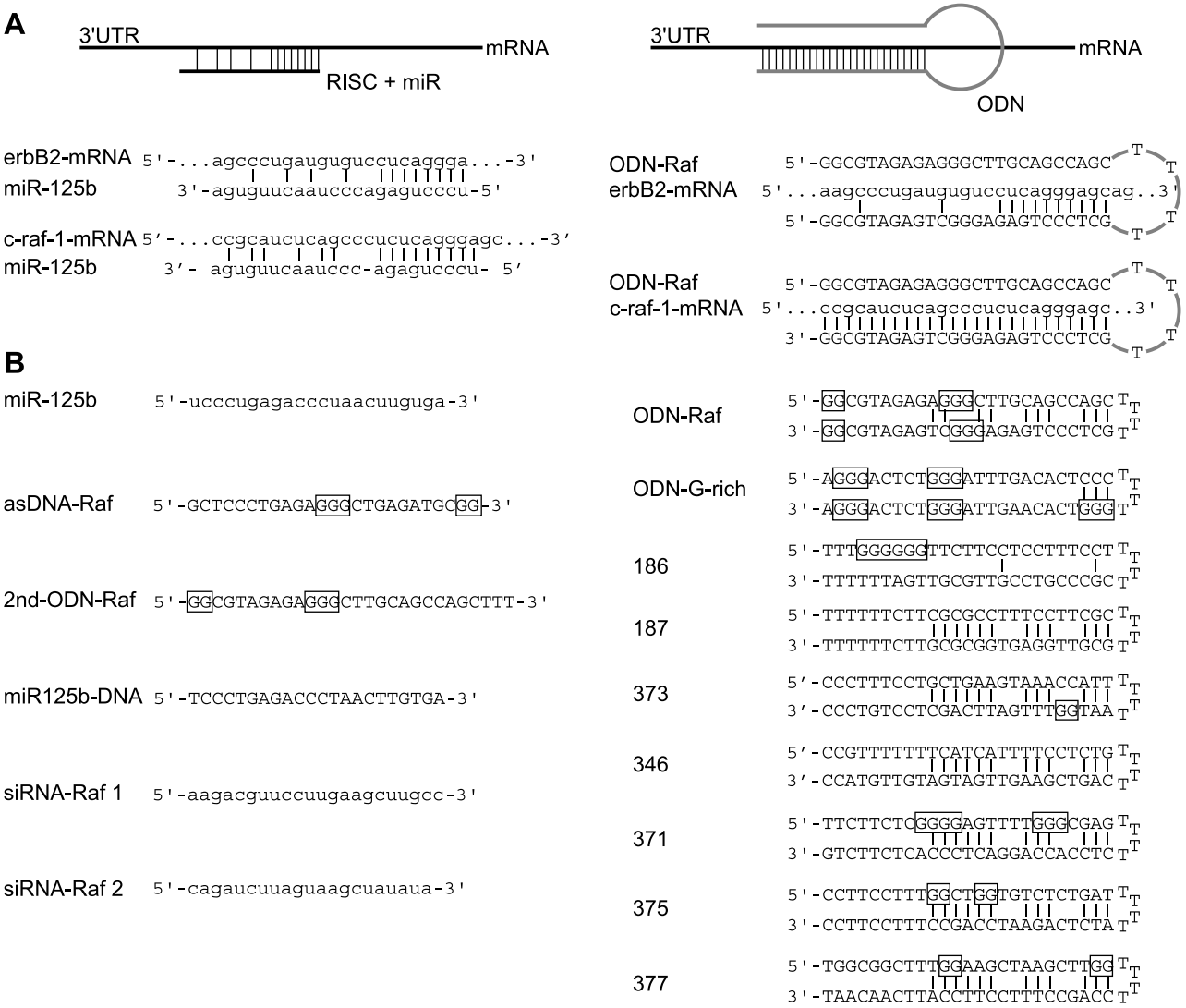

FIGURE 1. Sequences of ODNs, miR-125b, asDNA, and siRNAs. **A.** The theoretical binding of processed miR-125b (22 nt) or short hairpin ODN-Raf (54 nt) to the 3′UTR region of c-raf-1 or erbB2 mRNA is visualized. Vertical lines, Watson-Crick base pairs. The c-raf-1 sequence (NG_007467) and erbB2 sequence (NM_004448) were used for specific ODN-Raf design. RNA sequences are shown in lowercase letters and DNA sequences in capitals. **B.** Sequences of miR-125b, asDNA-Raf (25 nt), second strand of ODN-Raf (2nd-ODN-Raf; 28 nt), miR-125b-DNA (22 nt), siRNAs (21-22 nt; *left*), and ODNs (*right*) used in this study. ODNs consist of an antisense strand of 25 nt, a linker of 4 thymidines, and a second strand of 25 nt. All ODNs are phosphothioated at the three terminal nucleotides and the ODNs additionally in the T-linker. The antisense strand of ODN-Raf is fully complementary to the c-raf-1 mRNA sequence and partially complementary to erbB2 mRNA. Negative control ODNs are termed by numbers and G-tracts are boxed.

Effect of ODN-Raf on Survival

C-Raf is a survival factor, and downregulation of C-Raf or knockout of c-raf-1 can induce cell death (43). We investigated the effect of ODN-Raf on cell survival by performing an MTS assay. ODN-Raf reduced cell viability by 70% compared with negative controls (Fig. 7A). We then analyzed the induction of cleavage of poly-(ADP-ribose)-polymerase 1 (PARP-1) as a marker of cell death (44, 45). Cells transfected with 25 or 50 nmol/L ODN-Raf exhibited a 5- or 7-fold increased amount of cleaved PARP compared with cells transfected with the negative control 373 (Fig. 7B and C). Similarly effective were the positive control ODN-G-rich as well as 2nd-ODN-Raf. AsDNA-Raf induced PARP cleavage but to a weaker extent. SiRNA-Raf, miR-125b, miR-125b-DNA, and negative controls had no significant effect. Thus, PARP-cleavage on treatment with ODN-Raf may be attributed to its second strand, which might be partially explained by G-tetrad formation.

Discussion

In this study, we characterized the function of a short hairpin-looped ODN, which was targeted to c-raf-1 mRNA, and compared it with miR, asDNA, and siRNA. We have previously described such ODNs as activators of retroviral and cellular RNases H, leading to down-regulation of target RNAs in the presence of a viral RNase H, especially in the case of HIV in cell culture (18) and in patient-derived plasma (46), a model retrovirus in mice (19), and a lentivirus in the mouse vagina (47). We could also show that influenza virus production in lung cells and in the lungs of mice can be reduced by treatment with an ODN against influenza polymerase gene (48) possibly involving cellular RNases H. Also, growth of herpes simplex virus-1 could be inhibited by ODNs targeting essential herpes simplex virus-1 genes *in vitro* (49). We now asked whether short hairpin-looped ODNs can also target endogenous cellular mRNAs using the example of the proto-oncogene *c-raf-1*. The target site was selected based on the sequence of the previously described endogenous miR-125b targeting ErbB2, which we identified as a miR that potentially also regulates C-Raf. Overexpression of miR-125b in MDA-MB-453 cells clearly reduced Raf and ErbB2 levels (Fig. 2D-F). The reduction of C-Raf by miR-125b is in agreement with the observed growth inhibitory response to miR-125b in

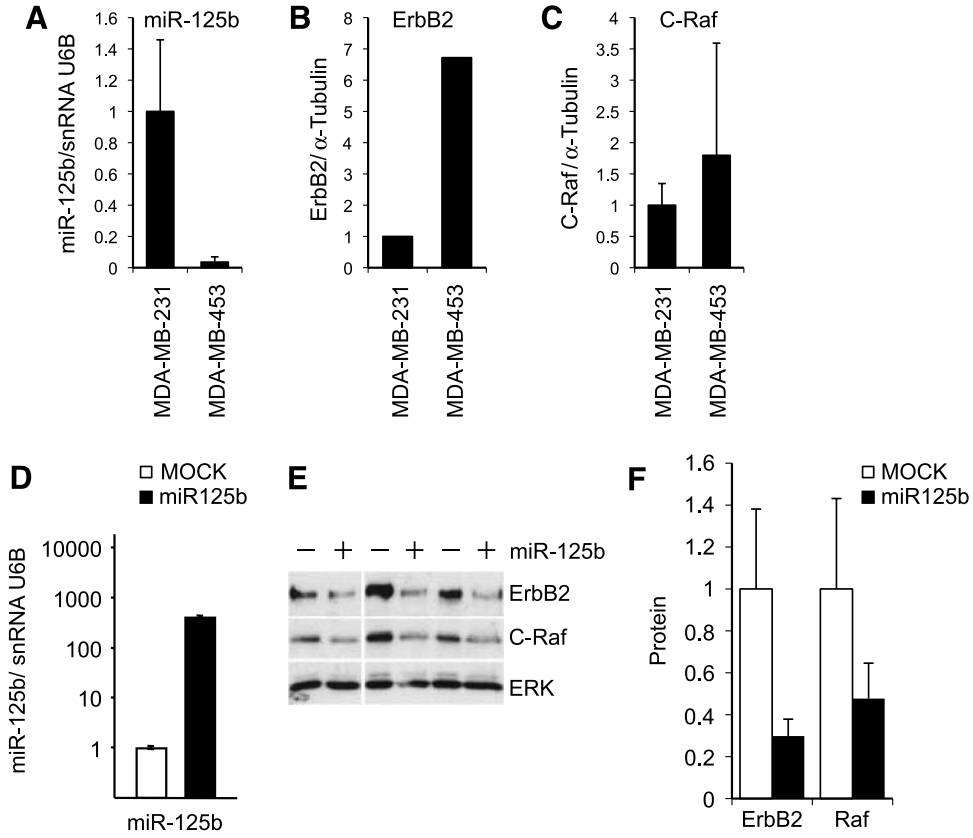

FIGURE 2. Effect of miR-125b on receptor tyrosine kinase ErbB2 and C-Raf expression. **A** to **C.** Endogenous levels of miR-125b, ErbB2, and C-Raf. MDA-MB-231 and MDA-MB-453 cells were grown to 90% confluency. **A.** MiRs were extracted and relative miR-125b levels normalized to snRNA U6B were determined by quantitative real-time RT-PCR. The values of MDA-MB-231 cells were arbitrarily set to 1. Columns, mean of two independent experiments; bars, SD. **B** and **C.** ErbB2 (**B**) and C-Raf (**C**) levels were determined by immunoblotting and densitometrically quantified. Five independent experiments were done for C-Raf. **D.** MDA-MB-453 cells were triple transfected at intervals of 24 h with 50 nmol/L miR-125b or mock transfected, and cells were lysed 24 h after the last transfection. MiR-125b levels were analyzed as in **A**. The values of untreated cells were arbitrarily set as 1. Columns, mean of two independent experiments; bars, SD. **E.** MDA-MB-453 cells were triple transfected at intervals of 24 h with 50 nmol/L miR-125b (+) and cells were lysed 24 h after the last transfection. Protein expression of ErbB2 and C-Raf was detected by immunoblotting. **F.** Relative amounts of proteins were quantified and normalized to the signal-regulated kinase protein (ERK2). Values of mock-transfected cells were set as 1. Columns, mean of three independent experiments; bars, SD.

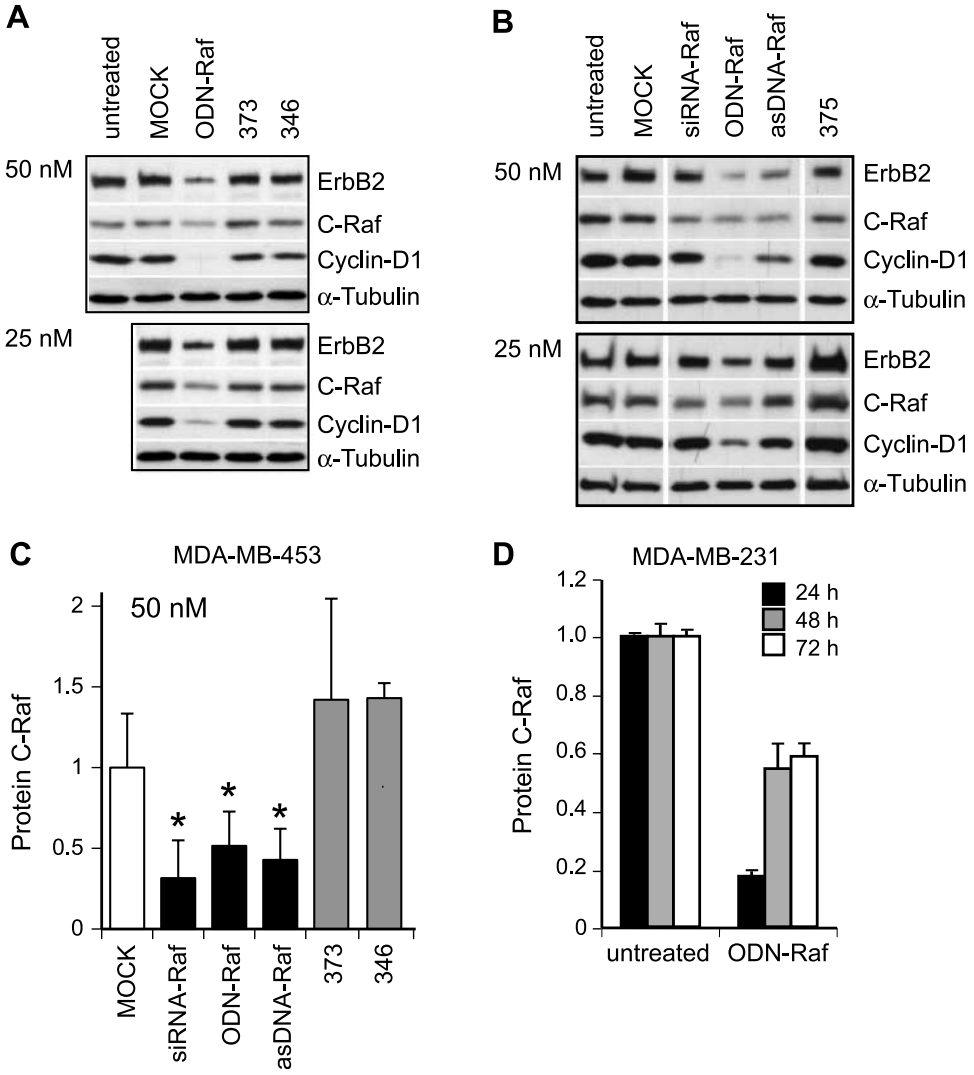

FIGURE 3. Effects of miR-125b, ODN, asDNA, and siRNA on C-Raf protein expression. **A** and **B.** MDA-MB-453 cells were transfected with the indicated oligonucleotides at a concentration of 25 or 50 nmol/L. Mock treatment was Lipofectamine 2000 alone. Protein levels of C-Raf, ErbB2, cyclin D1, and α-tubulin were analyzed 24 h after transfection by immunoblotting. **C.** Protein bands were densitometrically quantified, and relative amounts of C-Raf to α-tubulin calculated. Columns, relative protein levels from five independent experiments; bars, SD. *, $P < 0.05$, in comparison with mock. **D.** MDA-MB-231 cells were transfected with 500 nmol/L ODN-Raf and analyzed by immunoblotting after 24, 48, and 72 h. Columns, Raf levels from two independent experiments; bars, SD.

MCF10A breast epithelial cells independent of their ErbB2 status (30). MDA-MB-453 cells expressed less miR-125b than did MDA-MB-231 cells, and this correlated with a higher expression of ErbB2 and C-Raf (Fig. 2A-C). The increase in protein levels was much more pronounced for ErbB2 than for C-Raf. Given a comparable complementarity of miR-125b to both target sites on erbB2 and c-raf-1 mRNA (Fig. 1A) and a comparable accessibility of these target sites, we speculate that other cell type–specific mechanisms contribute to the strong overexpression of ErbB2 in MDA-MB-453 cells. Although gene amplification does not account for overexpression of ErbB2 in MDA-MB-453 cells (50), several other mechanisms (51) besides miR-125b are possible.

The reduction of C-Raf by miR-125b suggested that the target site of miR-125b on c-raf-1 is accessible for interfering oligonucleotides. We therefore designed ODN-Raf to target this site. The antisense strand of ODN-Raf was fully complementary to the 3′UTR region of c-raf-1 mRNA and 42% complementary to the 3′UTR region of erbB2 mRNA. The second strand was designed based on an HIV ODN (20) whereby the second strand was partially complementary to the antisense strand. This structure was superior to single-stranded asDNA, which may have been due to improved stability and possibly to secondary structures, which contributed to the antiviral effect (18, 20).[3]

Most asDNAs and ODNs activate RNases H, which cleave and degrade the RNA of DNA-RNA hybrids (15, 20, 52, 53).

[3] J. Heinrich and K. Moelling, unpublished results.

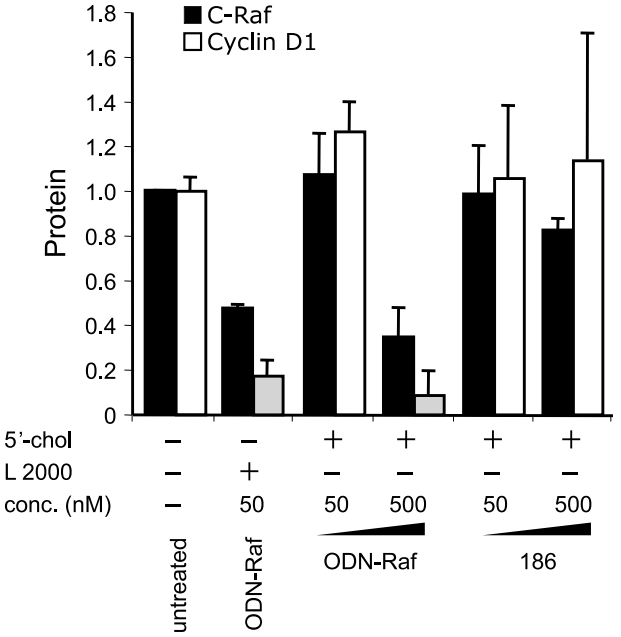

FIGURE 4. Effect of 5′-cholesterol–conjugated short hairpin-looped ODNs. MDA-MB-453 cells were transfected with ODN-Raf or control 186 at a concentration of 50 and 500 nmol/L. 5′-Cholesterol–modified or unmodified ODNs were either transfected with or without the transfection reagent Lipofectamine 2000 as indicated. Twenty-four hours after transfection, protein levels of C-Raf and cyclin D1 were determined by immunoblotting and densitometrically quantified. The relative amounts of C-Raf or cyclin D1 to α-tubulin were calculated. Values of untransfected cells were set as 1 and compared with transfected cells. Columns, mean of two independent experiments; bars, SD.

AsDNA can also block translation by steric hindrance of the ribosomes (14, 54, 55), and miRs primarily inhibit translation of proteins (13, 56). ODN-Raf as well as miR-125b did not lead to a reduction of c-raf-1 mRNA but reduced C-Raf protein levels by 50% (Figs. 3C and 5A). SiRNA-Raf resulted in a reduction of both c-raf-1 transcripts and C-Raf protein levels by ~70% (Figs. 3C and 5A). AsDNA-Raf reduced the protein level by 60% and the mRNA level by 25%. This suggests that ODN-Raf does not allow cleavage of c-raf-1 mRNA by recruitment of cellular RNases H but may interfere with translation, although we cannot exclude a contribution of a posttranslational mechanism. In addition, we observed that ODN-Raf reduced the expression of ErbB2 protein by ~50% to 60%. This can be explained by a stretch of 11 of 26 nt of ODN-Raf, which is complementary to the erbB2 mRNA.

Both ErbB2 and C-Raf can regulate the expression of cyclin D1, a key regulator of the G_1 checkpoint in the cell cycle (25, 57). Consistently, ODN-Raf diminished cyclin D1 level. SiRNA-Raf functioned more specifically than did ODN-Raf and reduced C-Raf but not ErbB2. SiRNA did not significantly decrease cyclin D1, indicating that Raf depletion is not sufficient for cyclin D1 reduction under these conditions. Additional downregulation of ErbB2 seems to be responsible for cyclin D1 decrease.

C-Raf is a survival factor that inhibits in a kinase-independent manner the proapoptotic kinases ASK1 (58) and MST2 (59). Knockout of C-Raf in mice or in C-Raf–deficient cells can cause Fas-induced apoptosis (43, 60). We observed that transfection of ODN-Raf led to a significant detachment of transfected cells and loss of viability as determined by an MTS assay. Cell death was confirmed by detection of cleaved PARP. Also in this case, siRNA-Raf was not sufficient, indicating that at least in MDA-MB-453 breast cancer cells, an additional function of ODN-Raf was essential to exert its effect. In agreement with this, antisense reagents against mRNAs of c-raf-1 or erbB2 have been described to inhibit proliferation, whereas for apoptosis, coadministration with mitotic inhibitors or DNA alkylating agents is required [Khazak et al. (29); Yang et al., 2003].

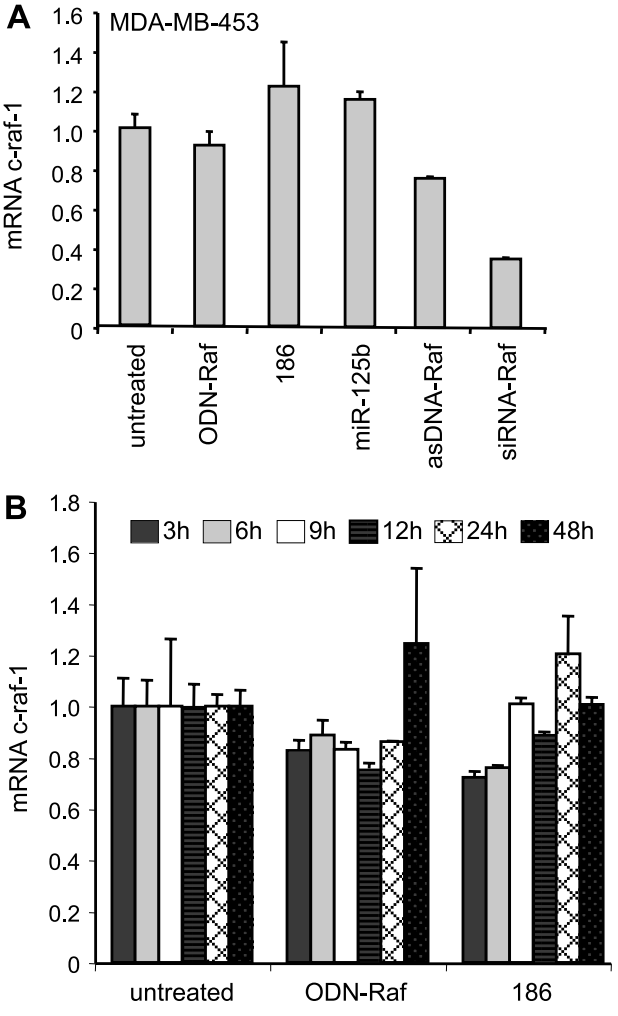

FIGURE 5. Effects of miR-125b, ODN, asDNA, and siRNA on c-raf-1 gene expression. **A.** MDA-MB-453 cells were transfected with miR-125b and oligonucleotides as indicated and lysed 24 h after transfection, and then total RNA was extracted. mRNA levels of c-raf-1 and β-actin were quantified by quantitative real-time RT-PCR, and mRNA of c-raf-1 was normalized to β-actin mRNA. **B.** MDA-MB-453 cells were transfected with ODN-Raf, miR-125b, or control ODNs as indicated or left untransfected and lysed at different times after transfection as indicated (3, 6, 9, 12, 24, and 48 h). Levels of c-raf-1 mRNA were quantified by quantitative real-time RT-PCR and were normalized to β-actin mRNA. **A** and **B.** Values of untransfected cells were set as 1 and compared with transfected cells. Columns, mean of two independent experiments; bars, SD.

The additional property in the case of ODN-Raf may depend on structural features. The antisense and the second strand of ODN-Raf consist of two GG and two GGG clusters in a motif, which would allow G-tetrad formation. Consistently, we detected higher-ordered structures of ODN-Raf, which are maintained following heat denaturation in the presence of Na^+ and K^+ ions but are lost in the presence of Li^+, suggesting that this band may represent G-tetrads (Fig. 6). Transfection with ODN-Raf and ODN-G-rich, which exhibit putative G-tetrads, induced cleavage of PARP and cell death. Also, 2nd-ODN-Raf and, more weakly, asDNA-Raf induced PARP-cleavage and cell death. Both single-stranded ODNs contain a GGG string and a GG string and might be able to form intermolecular G-tetrads. However, other mechanisms cannot be excluded thus far. One might speculate that reduced C-Raf expression and inhibition of the ERK pathway further enhance this effect.

To enhance the transfection efficiency and to replace transfection reagents *in vivo*, 3′-cholesterol–modified oligonucleotides have been used (39, 61). In the present study, we showed that a 5′-cholesterol modification allowed uptake without a transfection reagent but required a 10-fold higher concentration to achieve similar effects (Fig. 4). Despite this reduced efficiency, the cholesterol modification might be advantageous to overcome toxicity of transfection reagents. Furthermore, other modifications may be useful to further improve ODN-Raf.

In conclusion, our data show that a short hairpin-looped ODN-Raf molecule, which has a fully complementary antisense strand to the potential target site of miR-125b in the 3′UTR of c-raf-1, reduces the endogenous C-Raf protein level and, indirectly, cyclin D1 protein expression. Because ODN-Raf also affects ErbB2 due to a partially complementary sequence, this may also influence the expression of cyclin D1 through the ERK pathway. These negative regulatory effects of ODN-Raf are comparable to those of miR-125b. However, ODN-Raf also induces cell death, which might be attributed to both a reduction of Raf levels and the structural properties of ODN-Raf, such as the possibility to form G-tetrads. Thus, the described short-hairpin looped ODN-Raf is a multifunctional molecule that decreases the levels of oncogene proteins and stimulates cell death. Both effects are favorable to interfere with tumor growth. ODNs could be used as an alternative approach in further investigations to reduce oncogenic signaling in tumor cells.

Materials and Methods

Oligonucleotides

Hsa-miR-125b, which yields miR-125b on processing in the cell, was purchased from Dharmacon; all ODNs and asDNAs were from Metabion; and 5′-cholesterol–modified ODNs was from IBA. The two validated siRNAs (Hs_Raf1_6 and Hs_Raf1_5; Qiagen) used in this study target a region different than the 3′UTR of c-raf-1. All sequences are shown in Fig. 1B.

Cell Culture and Transfection

MDA-MB-453 and MDA-MB-231 breast cancer cell lines were obtained from the American Type Culture Collection and were cultivated in DMEM supplemented with 10% FCS.

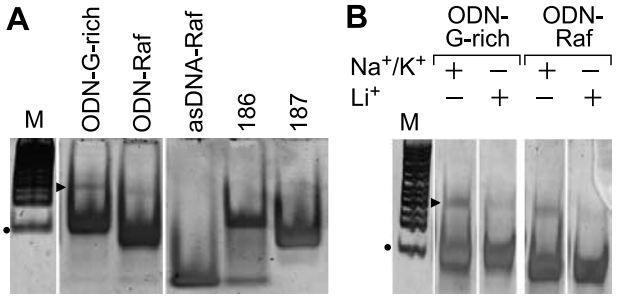

FIGURE 6. Secondary structure of ODN-Raf. **A.** Two hundred nanograms of ODN-Raf, control ODNs, and asDNA, diluted in 1× PBS, were analyzed by native 10% PAGE. Arrowhead, faint bands representing higher-ordered structures. M, 50 bp ladder; the dot indicates 50 bp. All lanes are from one gel. **B.** To analyze the stability of the higher-ordered structures, ODN-Raf and ODN-G-rich were heat denatured for 5 min at 95°C in either 1× PBS (Na^+/K^+) or 100 mmol/L LiCl pH 6.6 (Li^+) and quickly cooled down to 4°C. Denatured ODNs (200 ng) were analyzed on a 10% polyacrylamide. All lanes are from one gel.

Two hours before transfection, cells were seeded into six-well plates (4×10^5 per well with 2 mL of DMEM containing 10% FCS). Lipofectamine 2000 (Invitrogen Corp.) was used to transfect ODNs, asDNAs, or siRNAs. The transfection mixture was set up in a final volume of 160 μL and included 4 μL of Lipofectamine 2000, OptiMEM (Invitrogen), and the respective oligonucleotide for a final concentration of 50 or 500 nmol/L in the well. HighPerfect (Qiagen) was used to transfect miR-125b. The transfection mix was set up in a final volume of 100 μL and included 12 μL of HighPerfect, OptiMEM, and the respective oligonucleotide for a final concentration of 50 nmol/L in the well. 5′-Cholesterol–modified ODNs were transfected without using a transfection reagent. The prediluted mixture of 80 μL was incubated at room temperature for 15 min and added to the cells. Four hours after transfection, the medium was changed to fresh growth medium.

Preparation of RNA and miRs

Cells were washed twice with ice-cold PBS (137 mmol/L NaCl, 10 mmol/L phosphate, 2.7 mmol/L KCl, pH 7.4) and harvested in 250 μL of RLT lysis buffer (Qiagen) for total RNA extraction. For RNA preparation, the RLT cell suspension was loaded onto shredder columns (Qiagen) and RNA was prepared using the RNeasy Mini Kit (Qiagen) according to the supplier's instructions. Each sample was reverse transcribed using 250 ng of RNA, random hexamers, and the TaqMan High Capacity cDNA Kit (Applied Biosystems). Reverse transcription was carried out at 25°C for 10 min, 37°C for 2 h, and 70°C for 10 min.

MiR was extracted from cells using the miRVana miRNA Isolation Kit (Ambion) according to the supplier's instruction. Extracted miRs were measured with the Nanodrop 1000 Spectrophotometer (NanoDrop Technologies) and adjusted to 20 ng/μL. For miR-125b and small nuclear RNA (snRNA) U6B, reverse transcription was done in a total volume of 10 μL using 20 ng of miRs, the miRVana qRT-PCR Detection Kit (Applied Biosystems), and specific qRT-PCR primers (Applied Biosystems) for either miR-125b or snRNA U6B (NR_002752) according to the supplier's instructions. Reactions were incubated at 37°C for 30 min and 95°C for 10 min.

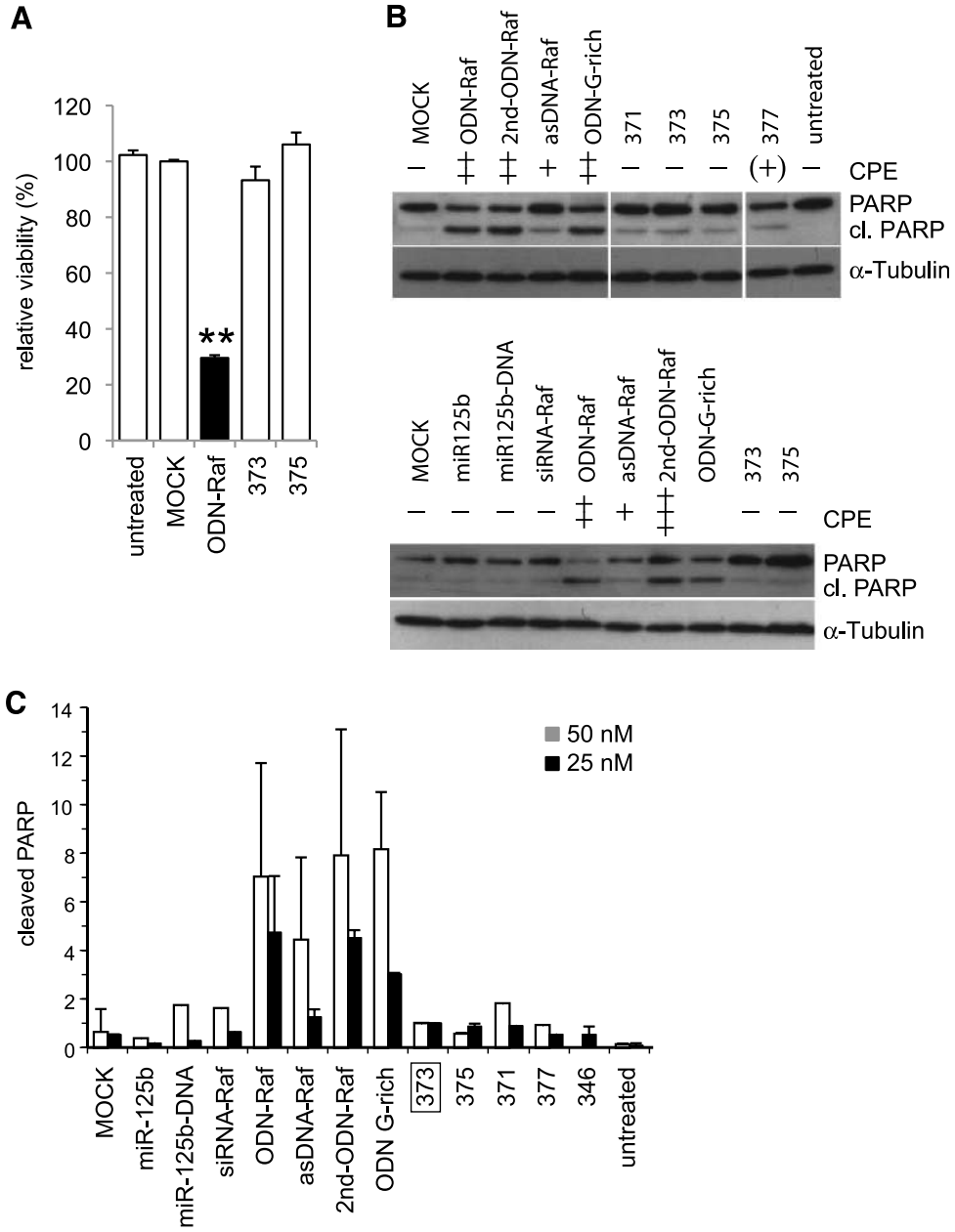

FIGURE 7. Effect on cell viability and PARP cleavage. **A** to **C.** MDA-MB-453 cells were transfected with 25 nmol/L of the indicated oligonucleotides and analyzed 24 h later. **A.** Effect on cell viability determined by an MTS assay. **B.** Cleavage of PARP was analyzed by immunoblotting. Two experiments are shown. In each blot, all lanes are from one gel. The cytopathic effect (*CPE*) determined by visual inspection is indicated. **C.** The intensities of the bands representing cleaved PARP were determined by densitometric analysis, normalized to α-tubulin, and expressed as fold increase in comparison with the 373-treated control (*boxed*). The graph summarizes five independent experiments with 2 to 5 points per oligonucleotide in total.

Quantitative Real-time RT-PCR

Relative mRNA expression levels were quantified using the transcribed cDNA and a commercially available quantitative real-time RT-PCR TaqMan assay (Applied Biosystems) on an ABI Prism 7500 system (Applied Biosystems). For normalization, a predeveloped β-actin TaqMan assay was used (Applied Biosystems). The amplification was carried out at 50°C for 2 min, 95°C for 10 min, and 50 cycles with 15 s at 95°C and 1 min at 60°C.

The miR expression levels were quantified using the specifically reverse transcribed cDNA, the miRVana qRT-PCR Primer Set for either miR-125 or snRNA U6B (Applied Biosystems), the miRVana qRT-PCR miRNA Detection Kit (Applied Biosystems), and the ABI Prism 7500 system (Applied Biosystems) according to the supplier's instructions. The level of miR-125b was normalized to snRNA U6B (62). SYBR Green I (Sigma-Aldrich), a nucleic acid stain, was used for real-time monitoring of miR expression.

A dilution row of miR-125b (Dharmacon) was used as positive control.

Protein Preparation and Analysis of Protein Expression

Cells were harvested in PBS and centrifuged for 1 min at 13,000 rpm. For Figs. 3 and 7, adherent and floating cells were harvested. The pellet was resuspended in 75 μL of lysis buffer [50 mmol/L Tris-HCl (pH 7.5), 150 mmol/L NaCl, 1% NP40 (v/v), 1 mmol/L EDTA (pH 8.0), 2 mmol/L sodium vanadate, 25 mmol/L NaF, complete mini protease inhibitor from Roche] and incubated for 30 min on ice. The lysate was centrifuged for 2 min at 13,000 rpm. The protein amount was determined using the Bradford method (Bio-Rad). For immunoblotting, the following antibodies were used: anti–extracellular signal-regulated kinase 2 (anti-ERK2), anti–cyclin D1, anti–Raf-1, anti–α-tubulin (all from SantaCruz Biotechnology, Inc.), anti-PARP, and anti–phospho-stress-activated protein kinase/c-jun NH_2-terminal kinase (Cell Signalling Technology, Inc.). Bound antibodies were detected by using peroxidase-labeled secondary antibodies (SantaCruz Biotechnology) and immunoblotting and enhanced chemiluminescence detection reagents from Amersham. Scanned immunoblots were analyzed using the image software ImageQuant 5.2 (GE Healthcare).

Analysis of Secondary Structure

To analyze the short hairpin DNAs and potential secondary structures, native 10% polyacrylamide gels were used. Two hundred nanograms of ODN-Raf, control ODNs, and asDNA diluted in 1×PBS were analyzed with a 10% polyacrylamide gel, which was stained with SYBR Green 2 for 10 min and analyzed on a fluorescence imaging system Storm 860 Molecular Imager (GMI, Inc.).

MTS Assay

The effect of ODNs on cell viability was determined by the CellTiter 96 Aqueaous One Solution Cell Proliferation Assay (Promega) using MTS. Cells were seeded in triplicate in a 48-well plate and transfected as described above, and then MTS assay was done according to the manufacturer's instructions 24 h after transfection. The relative viability was calculated by comparison with mock-transfected cells.

Disclosure of Potential Conflicts of Interest

No potential conflicts of interest were disclosed.

Acknowledgments

We thank Dr. Anja Twiehaus and Farahmand Firouzeh for excellent technical assistance, especially for performing qRT-PCR experiments.

References

1. Bartel DP. MicroRNAs: genomics, biogenesis, mechanism, and function. Cell 2004;116:281–97.

2. Boyd SD. Everything you wanted to know about small RNA but were afraid to ask. Lab Invest 2008;88:569–78.

3. Iorio MV, Ferracin M, Liu CG, et al. MicroRNA gene expression deregulation in human breast cancer. Cancer Res 2005;65:7065–70.

4. Verghese ET, Hanby AM, Speirs V, Hughes TA. Small is beautiful: microRNAs and breast cancer—where are we now? J Pathol 2008;215:214–21.

5. Kloosterman WP, Plasterk RH. The diverse functions of microRNAs in animal development and disease. Dev Cell 2006;11:441–50.

6. Stenvang J, Kauppinen S. MicroRNAs as targets for antisense-based therapeutics. Expert Opin Biol Ther 2008;8:59–81.

7. Rayburn ER, Zhang R. Antisense, RNAi, and gene silencing strategies for therapy: mission possible or impossible? Drug Discov Today 2008;13:513–21.

8. Ross JS, Carlson JA, Brock G. miRNA: the new gene silencer. Am J Clin Pathol 2007;128:830–6.

9. Scherer LJ, Rossi JJ. Approaches for the sequence-specific knockdown of mRNA. Nat Biotechnol 2003;21:1457–65.

10. Soifer HS, Rossi JJ, Saetrom P. MicroRNAs in disease and potential therapeutic applications. Mol Ther 2007;15:2070–9.

11. Aagaard L, Rossi JJ. RNAi therapeutics: principles, prospects and challenges. Adv Drug Deliv Rev 2007;59:75–86.

12. Dean NM. Functional genomics and target validation approaches using antisense oligonucleotide technology. Curr Opin Biotechnol 2001;12:622–5.

13. Shyu AB, Wilkinson MF, van Hoof A. Messenger RNA regulation: to translate or to degrade. EMBO J 2008;27:471–81.

14. Cohen JS. Selective anti-gene therapy for cancer: principles and prospects. Tohoku J Exp Med 1992;168:351–9.

15. Dash P, Lotan I, Knapp M, Kandel ER, Goelet P. Selective elimination of mRNAs *in vivo*: complementary oligodeoxynucleotides promote RNA degradation by an RNase H-like activity. Proc Natl Acad Sci U S A 1987;84:7896–900.

16. Jendis J, Strack B, Moelling K. Inhibition of replication of drug-resistant HIV type 1 isolates by polypurine tract-specific oligodeoxynucleotide TFO A. AIDS Res Hum Retroviruses 1998;14:999–1005.

17. Jendis J, Strack B, Volkmann S, Boni J, Molling K. Inhibition of replication of fresh HIV type 1 patient isolates by a polypurine tract-specific self-complementary oligodeoxynucleotide. AIDS Res Hum Retroviruses 1996;12:1161–8.

18. Matskevich AA, Ziogas A, Heinrich J, Quast SA, Moelling K. Short partially double-stranded oligodeoxynucleotide induces reverse transcriptase/RNase H-mediated cleavage of HIV RNA and contributes to abrogation of infectivity of virions. AIDS Res Hum Retroviruses 2006;22:1220–30.

19. Matzen K, Elzaouk L, Matskevich AA, Nitzsche A, Heinrich J, Moelling K. RNase H-mediated retrovirus destruction *in vivo* triggered by oligodeoxynucleotides. Nat Biotechnol 2007;25:669–74.

20. Moelling K, Abels S, Jendis J, Matskevich A, Heinrich J. Silencing of HIV by hairpin-loop-structured DNA oligonucleotide. FEBS Lett 2006;580:3545–50.

21. Garzon R, Fabbri M, Cimmino A, Calin GA, Croce CM. MicroRNA expression and function in cancer. Trends Mol Med 2006;12:580–7.

22. Tavazoie SF, Alarcon C, Oskarsson T, et al. Endogenous human microRNAs that suppress breast cancer metastasis. Nature 2008;451:147–52.

23. Liu X, Yan S, Zhou T, Terada Y, Erikson RL. The MAP kinase pathway is required for entry into mitosis and cell survival. Oncogene 2004;23:763–76.

24. Hilger RA, Scheulen ME, Strumberg D. The Ras-Raf-MEK-ERK pathway in the treatment of cancer. Onkologie 2002;25:511–8.

25. Kerkhoff E, Rapp UR. Cell cycle targets of Ras/Raf signalling. Oncogene 1998;17:1457–62.

26. Kolch W. Meaningful relationships: the regulation of the Ras/Raf/MEK/ERK pathway by protein interactions. Biochem J 2000;351 Pt 2:289–305.

27. Moelling K, Strack B, Radziwill G. Signal transduction as target of gene therapy. Recent Results Cancer Res 1996;142:63–71.

28. Roberts PJ, Der CJ. Targeting the Raf-MEK-ERK mitogen-activated protein kinase cascade for the treatment of cancer. Oncogene 2007;26:3291–310.

29. Khazak V, Astsaturov I, Serebriiskii IG, Golemis EA. Selective Raf inhibition in cancer therapy. Expert Opin Ther Targets 2007;11:1587–609.

30. Scott GK, Goga A, Bhaumik D, Berger CE, Sullivan CS, Benz CC. Coordinate suppression of ERBB2 and ERBB3 by enforced expression of micro-RNA miR-125a or miR-125b. J Biol Chem 2007;282:1479–86.

31. Ghosh MK, Cohen JS. Oligodeoxynucleotides as antisense inhibitors of gene expression. Prog Nucleic Acid Res Mol Biol 1992;42:79–126.

32. Tuschl T, Borkhardt A. Small interfering RNAs: a revolutionary tool for the analysis of gene function and gene therapy. Mol Interv 2002;2:158–67.

33. Mazumder B, Seshadri V, Fox PL. Translational control by the 3′-UTR: the ends specify the means. Trends Biochem Sci 2003;28:91–8.

34. Si ML, Zhu S, Wu H, Lu Z, Wu F, Mo YY. miR-21-mediated tumor growth. Oncogene 2007;26:2799–803.

35. Krueger U, Bergauer T, Kaufmann B, et al. Insights into effective RNAi gained from large-scale siRNA validation screening. Oligonucleotides 2007;17:237–50.

36. Baldin V, Lukas J, Marcote MJ, Pagano M, Draetta G. Cyclin D1 is a nuclear protein required for cell cycle progression in G_1. Genes Dev 1993;7:812–21.

37. Quelle DE, Ashmun RA, Shurtleff SA, et al. Overexpression of mouse D-type cyclins accelerates G_1 phase in rodent fibroblasts. Genes Dev 1993;7: 1559–71.

38. Krutzfeldt J, Rajewsky N, Braich R, et al. Silencing of microRNAs *in vivo* with "antagomirs". Nature 2005;438:685–9.

39. Margineanu A, De Feyter S, Melnikov S, et al. Complexation of Lipofectamine and cholesterol-modified DNA sequences studied by single-molecule fluorescence techniques. Biomacromolecules 2007;8:3382–92.

40. Olsen PH, Ambros V. The lin-4 regulatory RNA controls developmental timing in *Caenorhabditis elegans* by blocking LIN-14 protein synthesis after the initiation of translation. Dev Biol 1999;216:671–80.

41. Seggerson K, Tang L, Moss EG. Two genetic circuits repress the *Caenorhabditis elegans* heterochronic gene lin-28 after translation initiation. Dev Biol 2002; 243:215–25.

42. Creze C, Rinaldi B, Haser R, Bouvet P, Gouet P. Structure of a d(TGGGGT) quadruplex crystallized in the presence of Li+ ions. Acta Crystallogr D Biol Crystallogr 2007;63:682–8.

43. Galabova-Kovacs G, Kolbus A, Matzen D, et al. ERK and beyond: insights from B-Raf and Raf-1 conditional knockouts. Cell Cycle 2006;5:1514–8.

44. Cepeda V, Fuertes MA, Castilla J, et al. Poly(ADP-ribose) polymerase-1 (PARP-1) inhibitors in cancer chemotherapy. Recent Patents Anticancer Drug Discov 2006;1:39–53.

45. Soldani C, Scovassi AI. Poly(ADP-ribose) polymerase-1 cleavage during apoptosis: an update. Apoptosis 2002;7:321–8.

46. Heinrich J, Mathur S, Matskevich AA, Moelling K. Oligonucleotide-mediated retroviral RNase H activation leads to reduced HIV-1 titer in patient-derived plasma. AIDS 2009;23:213–21.

47. Wittmer-Elzaouk L, Jung-Shiu J, Heinrich J, Moelling K. Retroviral self-inactivation in the mouse vagina induced by short DNA. Antiviral Res 2009; 82:22–8.

48. Kwok T, Helfer H, Alam MI, Heinrich J, Pavlovic J, Moelling K. Inhibition of influenza A virus replication by short double-stranded oligodeoxynucleotides. Arch Virol 2009;154:109–14.

49. Falkenhagen A, Heinrich J, Moelling K. Short hairpin-loop-structured oligodeoxynucleotides reduce HSV-1 replication. J Virol 2009;6:43.

50. Kury FD, Schneeberger C, Sliutz G, et al. Determination of HER-2/neu amplification and expression in tumor tissue and cultured cells using a simple, phenol free method for nucleic acid isolation. Oncogene 1990;5:1403–8.

51. Mehta A, Trotta CR, Peltz SW. Derepression of the Her-2 uORF is mediated by a novel post-transcriptional control mechanism in cancer cells. Genes Dev 2006;20:939–53.

52. Moelling K, Bolognesi DP, Bauer H, Busen W, Plassmann HW, Hausen P. Association of viral reverse transcriptase with an enzyme degrading the RNA moiety of RNA-DNA hybrids. Nat New Biol 1971;234:240–3.

53. Toulme JJ, Verspieren P, Boiziau C, Loreau N, Cazenave C, Thuong NT. [Antisense oligonucleotides: tools of molecular genetics and therapeutic agents]. Ann Parasitol Hum Comp 1990;65 Suppl 1:11–4.

54. Kurreck J. Antisense technologies. Improvement through novel chemical modifications. Eur J Biochem 2003;270:1628–44.

55. Popescu FD. Antisense- and RNA interference-based therapeutic strategies in allergy. J Cell Mol Med 2005;9:840–53.

56. Wu L, Belasco JG. Let me count the ways: mechanisms of gene regulation by miRNAs and siRNAs. Mol Cell 2008;29:1–7.

57. Lavoie JN, Rivard N, L'Allemain G, Pouyssegur J. A temporal and biochemical link between growth factor-activated MAP kinases, cyclin D1 induction and cell cycle entry. Prog Cell Cycle Res 1996;2:49–58.

58. Chen J, Fujii K, Zhang L, Roberts T, Fu H. Raf-1 promotes cell survival by antagonizing apoptosis signal-regulating kinase 1 through a MEK-ERK independent mechanism. Proc Natl Acad Sci U S A 2001;98:7783–8.

59. O'Neill E, Rushworth L, Baccarini M, Kolch W. Role of the kinase MST2 in suppression of apoptosis by the proto-oncogene product Raf-1. Science 2004;306: 2267–70.

60. Leicht DT, Balan V, Kaplun A, et al. Raf kinases: function, regulation and role in human cancer. Biochim Biophys Acta 2007;1773:1196–212.

61. Krutzfeldt J, Kuwajima S, Braich R, et al. Specificity, duplex degradation and subcellular localization of antagomirs. Nucleic Acids Res 2007;35: 2885–92.

62. Ramkissoon SH, Mainwaring LA, Sloand EM, Young NS, Kajigaya S. Nonisotopic detection of microRNA using digoxigenin labeled RNA probes. Mol Cell Probes 2006;20:1–4.